Effects of interface phonon scattering in three-interface heterostructures

Mikhail V. Kisin
Department of Electrical Engineering, State University of New York at Stony Brook, Stony Brook, New York 11794-2350

Michael A. Stroscio
U.S. Army Research Office, P.O. Box 12211, Research Triangle Park, North Carolina 27709-2211

Gregory Belenky,[a] Vera B. Gorfinkel, and Serge Luryi
Department of Electrical Engineering, State University of New York at Stony Brook, Stony Brook, New York 11794-2350

(Received 24 November 1997; accepted for publication 10 January 1998)

A detailed study of the electron–optical–phonon interaction in an asymmetric one-well/one-barrier heterostructure is given. Dispersion relations and phonon potential distributions for interface phonon modes are derived in the framework of the macroscopic dielectric continuum model. It is found that for intrawell relaxation processes the sum of the scattering rates by all interface polar-optical phonon modes is *approximately* independent of the width of the barrier layer. Consequently, a simplified Hamiltonian for electron–phonon interaction in a single quantum well can be used for scattering rate calculation in multiple heterointerface structures. The combined scattering rates by interface and confined phonon modes are compared with the results obtained in an idealized model using the bulklike phonon spectrum. The practical invalidity of the latter approximation is shown for electron kinetic energies comparable with the typical energy of optical phonons in the heterostructure. © *1998 American Institute of Physics.* [S0021-8979(98)04308-4]

I. INTRODUCTION

Polar interaction with long-wavelength longitudinally polarized optical (LO) phonons is a topic of continuing interest, since electron inter- and intrasubband relaxation in quantum well heterostructures are governed primarily by this scattering mechanism. During the last decade, the importance of optical phonon confinement and localization effects has been discussed widely in literature. Both macroscopic[1–10] and microscopic[11–13] approaches of electron–optical–phonon interactions have been used to show that in polar semiconductor heterostructures, the interaction of confined electrons with polar-optical phonons is modified strongly compared to the three-dimensional case. The LO phonon scattering was shown to be important in narrow quantum well heterostructures designed for injection[5,6] or optically pumped[7,8] laser applications. Photoexcited carrier relaxation processes in coupled quantum wells[7] and phonon-assisted tunneling in double-barrier heterostructures[9] were described successfully taking into account the existence of interface optical-phonon modes.

All of the above treatments applied to highly symmetric structures such as quantum wells,[1–6] double-well,[7] or double-barrier heterostructures.[9,10] Recently, another kind of heterostructure has appeared in which an accurate description of the electron–optical–phonon interaction is of prime importance. The active region of the unipolar quantum cascade laser[14,15] incorporates a combination of a quantum well with an adjacent narrow barrier layer providing the electron tunneling escape from the active quantum well after a light-emitting transition (see Fig. 1). For this three-interface configuration, the interface phonon potential distributions should differ substantially from the well known solutions for symmetric heterostructures with an even number of interfaces.[2,5,10] In the latter case, the phonon potential distributions usually are characterized by definite parity providing well-known parity selection rules for electron inter- and intrasubband transitions.[2,4] In a three-interface heterostructure with a sufficiently narrow barrier layer, the parity based selection rules do not hold for intrawell electron transitions. This circumstance, combined with the growing complexity of the spectrum of interface optical phonon modes in multiple heterointerface structures,[16] gives rise to substantial difficulties in theoretical analysis of electron relaxation processes. In this article, we show that the total scattering rate by interface phonons in three-interface heterostructures is practically independent of the barrier width; this permit us to use the phonon spectrum of a single quantum well for the description of more complex cascade heterostructures.[6] Simultaneously, we show that any attempt to exploit the simpler bulklike phonon spectrum fails if the electron kinetic energy is of the order of the typical phonon energy in the heterostructure. The macroscopic dielectric continuum model[2] is used in this article for a description of the polar–optical–phonon modes; this has been shown to agree well with microscopic calculations.[11–13]

II. MODEL

We consider the simplest three-interface combination of a quantum well with an adjacent narrow barrier layer as in Fig. 1. Index $i=0\div 3$ numerates here the layers of the het-

[a]Electronic mail: garik@sbee.sunysb.edu

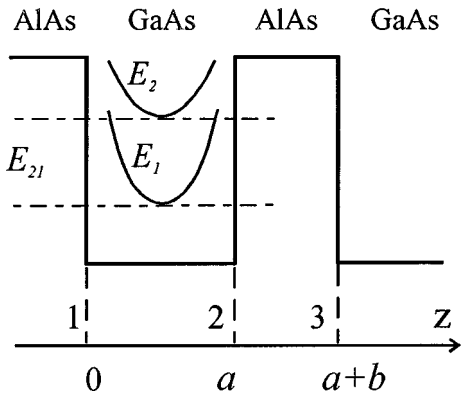

FIG. 1. Schematic plot of conduction band profile of the three-interface heterostructure discussed in this study.

erostructure. In cascade laser heterostructures, layers 0 and 3 represent the same layer which can be designed as a gradual alloy[14] or a superlattice.[15] Under an applied electric field, this layer provides a flatband condition for electron transport from one cascade to the next. The length of this region is usually longer then the active quantum well width, a, and its exact structure does not influence the intrawell electron relaxation processes considered in this article. Therefore, we represent the layers 0 and 3 as half-spaces of wide-gap and narrow-gap semiconductors, respectively.

In the dielectric continuum model, the optical phonon spectrum of a heterostructure includes interface phonon modes and confined LO phonon modes which are approximated as being completely confined to the corresponding layer (well or barrier) and not affected by or coupled to the adjacent layer.[1–3] The frequency of each interface mode is split according to different frequency ranges of optical phonons in the constituent materials. This splitting is influenced also by the type of materials used in the heterostructure which usually are binary materials or ternary alloys.[17] For the sake of simplicity, we consider here a binary material heterostructure assuming GaAs as the well material and AlAs as the barrier, wide-gap semiconductor. The relevant physical parameters used in numerical calculations are shown in Table I.

In the case of binary materials, the dielectric functions in the barrier (b) and the well (w) heterostructure layers are

$$\varepsilon_{b,w}(\omega)=\varepsilon_{b,w\infty}\frac{\omega^2-\omega_{lb,w}^2}{\omega^2-\omega_{tb,w}^2}. \tag{1}$$

TABLE I. Electron and phonon spectrum parameters of the three interface heterostructure.

Phonon spectrum		Electron spectrum	
$\hbar\omega_{lw}$	36.2 meV	m_c (GaAs)	0.067 m_0
$\hbar\omega_{tw}$	33.3 meV	E_g (GaAs)	1.4 eV
$\hbar\omega_{lb}$	50.1 meV	E_g (AlAs)	3.0 eV
$\hbar\omega_{tb}$	44.8 meV	$\Delta_c:\Delta_v$	6:4
$\varepsilon_{w\infty}$	10.9	E_{21}	225 meV
$\varepsilon_{b\infty}$	8.16		

Following the transfer matrix method described in Ref. 16, we can obtain the dispersion equation for a three-interface heterostructure in the form (see the Appendix):

$$\frac{\varepsilon_b(\omega)}{\varepsilon_w(\omega)}=\xi_m, \quad m=\text{outer,inner}, \tag{2}$$

where

$$\xi_{\text{outer}}=-1; \tag{3}$$

$$\xi_{\text{inner}(S,A)}=-\xi_0\pm\sqrt{\xi_0^2-1}$$

$$<0; \quad \xi_0=\frac{2}{(1-e^{2qa})(1-e^{-2qb})}-1. \tag{4}$$

Here, q is the in-plane phonon wave vector. Relations (2) and (3) give us two dispersionless solutions with constant frequencies equal to the frequencies of the two single-interface phonon modes of the GaAs/AlAs heterointerface. As we show below, these modes tend to localize in the vicinity of the outer heterointerfaces (1) or (3) and may be considered to be outer interface modes. Relations (2) and (4) in the limit $b\gg a$ lead to the dispersion equation of a simple double heterostructure (quantum well).[2,3] Consequently, we obtain two different types of inner modes which can be classified as symmetric (S) or antisymmetric (A) according to their behavior in this limit. In expression (4), the sign $(+)$ relates to the symmetric and the sign $(-)$ relates to the antisymmetric inner interface mode. By analogy with the outer mode, each inner mode is split in frequency according to the two optical phonon frequency ranges in constitutive materials. For binary materials, these dispersion relations can be easily obtained analytically by substituting dielectric functions (1) into the dispersion equation (2):

$$\omega_{m(b,w)}^2=\Omega_m^2\pm\left(\Omega_m^2-\frac{\omega_{lb}^2\omega_{tw}^2+\chi_m\omega_{lw}^2\omega_{tb}^2}{1+\chi_m}\right)^{1/2};$$

$$\begin{pmatrix} b \\ w \end{pmatrix}\rightarrow\begin{pmatrix} + \\ - \end{pmatrix}; \tag{5}$$

$$\Omega_m^2=\frac{\omega_{lb}^2+\omega_{tw}^2+\chi_m(\omega_{lw}^2+\omega_{tb}^2)}{2(1+\chi_m)}; \quad \chi_m=-\frac{\varepsilon_{w\infty}}{\varepsilon_{b\infty}}\xi_m>0.$$

Here, the sign $(+)$ corresponds to index b—that is to the phonon frequency range of barrier material—and the sign $(-)$ should be chosen for phonon frequency range of well material (index w). For ternary alloys, this classification scheme remains the same except for additional mode splitting. The calculated dispersion curves for interface phonon modes in a binary GaAs/AlAs heterostructure are presented in Fig. 2(a).

For a three-interface heterostructure, the interface phonon potential distributions can be found to have simple analytical form (see Appendix):

$$\varphi_{m,q}(z)=A_m\left(\frac{\hbar}{\varepsilon_0 q}\right)^{1/2}\left(\frac{\partial\varepsilon_b(\omega)}{\partial\omega}-\xi_m\frac{\partial\varepsilon_w(\omega)}{\partial\omega}\right)^{-1/2} f_m(z), \tag{6}$$

$$f(z)=\sum_{i=0}^{3}\left[C_{i1}e^{q(z_i-z)}+C_{i2}e^{q(z-z_{i+1})}\right]_{z_i<z<z_{i+1}}.$$

The coefficients in (6) are given by

$$A_{\text{outer}}=\left(\frac{e^{2qa}}{e^{2qa}+e^{2qb}-1}\right)^{1/2};\quad C_i=\begin{pmatrix}C_{i1}\\C_{i2}\end{pmatrix}; \tag{7}$$

$$C_0=\begin{pmatrix}0\\1\end{pmatrix};\quad C_1=\begin{pmatrix}1\\0\end{pmatrix};\quad C_2=\begin{pmatrix}0\\e^{q(b-a)}\end{pmatrix};\quad C_3=\begin{pmatrix}e^{q(b-a)}\\0\end{pmatrix}$$

for the outer interface mode and

$$A_{\text{inner}}=\left(\frac{1}{2}\frac{e^{2qb}-1}{e^{2qa}+e^{2qb}-1}\right)^{1/2};$$

$$C_0=\begin{pmatrix}0\\1\end{pmatrix};\quad C_1=\frac{1}{2}\begin{pmatrix}1-\xi\\(1+\xi)e^{qa}\end{pmatrix}; \tag{8}$$

$$C_2=\begin{pmatrix}(\xi+\xi_0)\sinh qa\\-e^{qa}\\\hline 2\sinh qb\end{pmatrix};\quad C_3=\begin{pmatrix}(\xi-1)e^{-qb}\sinh qa\\0\end{pmatrix}$$

for inner phonon modes. As in the case of one- and two-interface heterostructures, these distributions do not depend on the type of constitutive materials.[17] For ternary alloys, we simply have to use the two-pole approximation for the corresponding dielectric function (1). As a result, the introduction of a ternary alloy as a barrier or well material does not alter the functional form of the interface modes but modifies the coefficient for the mode strength according to the change in the dielectric function. The exemplary phonon potential distributions are presented in Fig. 3.

Figure 3(a) shows the characteristic behavior of the inner and outer optical-phonon modes in a three-interface heterostructure. In the limit $b\gg a$, the outer mode tends to localize on the right outer interface (3), whereas the inner modes relate to the well-known symmetric and antisymmetric interface modes in a double heterostructure.[2] If the barrier width, b, becomes comparable with well width, a, the inner modes are substantially perturbed but their basic symmetry features still remain; see Fig. 3(b). The outer mode now represents the symmetrized linear combination of the single interface modes of the left and right outer interfaces (1) and (3). If $a=b$, this combination is exactly symmetric. Further decrease of the barrier width b gives rise to a potential redistribution of the outer interface modes from interface (3 toward interface (1). At the same time, the inner phonon modes switch to the barrier layer, simultaneously changing their symmetry; see Fig. 3(c).

To characterize the individual phonon mode strengths, we can introduce the coupling coefficients, β_m, for the electron–phonon interactions, normalizing the phonon envelopes, $\varphi_m(z)$, in (6) according to the condition $\int\tilde{\varphi}^2(z)dz=1$. The interaction Hamiltonian is represented in the form

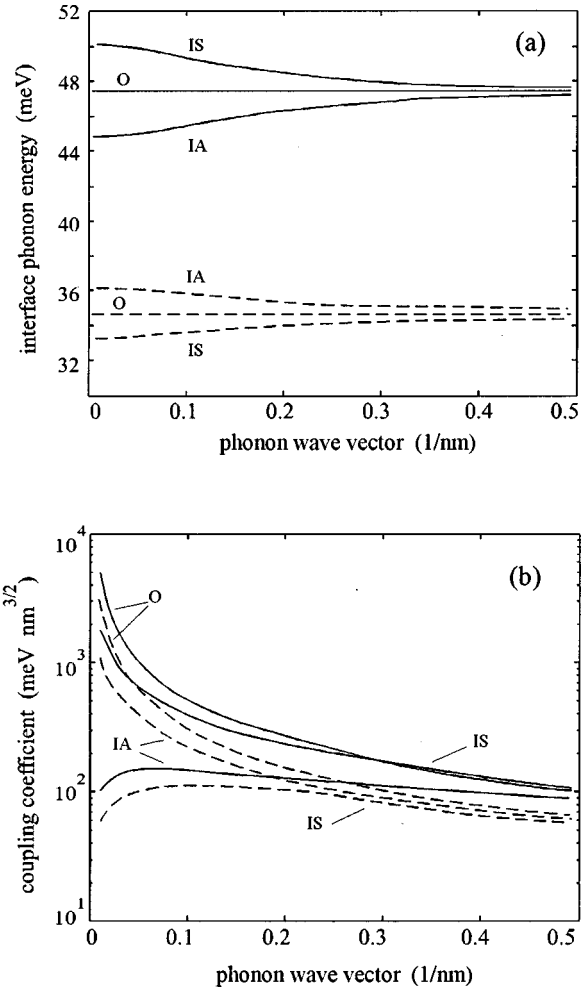

FIG. 2. Interface phonon mode (**a**) dispersions and (**b**) coupling constants for interface phonon modes in three-interface heterostructure with layer dimensions $a=6$ nm and $b=6$ nm. The interface modes are grouped into the GaAs-like (dashed lines) and AlAs-like (solid lines) modes in the ascending order in frequencies. There are three phonon modes in each group labeled by: I(O)—inner (outer) interface modes; S(A)—symmetric (antisymmetric) modes in the limit $b\gg a$.

$$H_{el-ph}=\sum_{m,\mathbf{q}}\beta_m(q)\tilde{\varphi}_{m,q}(z)\frac{e^{i\mathbf{qr}}}{\sqrt{S}}(\hat{a}_{m,\mathbf{q}}+\hat{a}^{+}_{m,-\mathbf{q}}). \tag{9}$$

Here, S is the cross-sectional area of the heterostructure. For non-normalized potentials (6), we would use the elementary electron charge, e, instead of coupling constants, β_m. The q dependence of β_m in the three-interface system is similar to that obtained in Ref. 9 for the case of a symmetric double-barrier heterostructure. The coupling constants of the outer interface modes (Ob, Ow) diverge as $1/q$ for small phonon wave vectors, q. The coupling constants for the LO-like inner phonon modes (IAw, ISb) diverge as $1/\sqrt{q}$, whereas for two TO-like inner modes (IAb, ISw) they tend to go to zero at small values of q. At larger q, all the coupling coefficients converge to the values of the corresponding coupling constant for the single interface mode in the phonon energy ranges of the barrier (b) or the well (w) semiconductor materials; see Fig. 2(b). However, the coupling constants by themselves cannot give us the most or the least important phonon modes in the scattering process. The overlap inte-

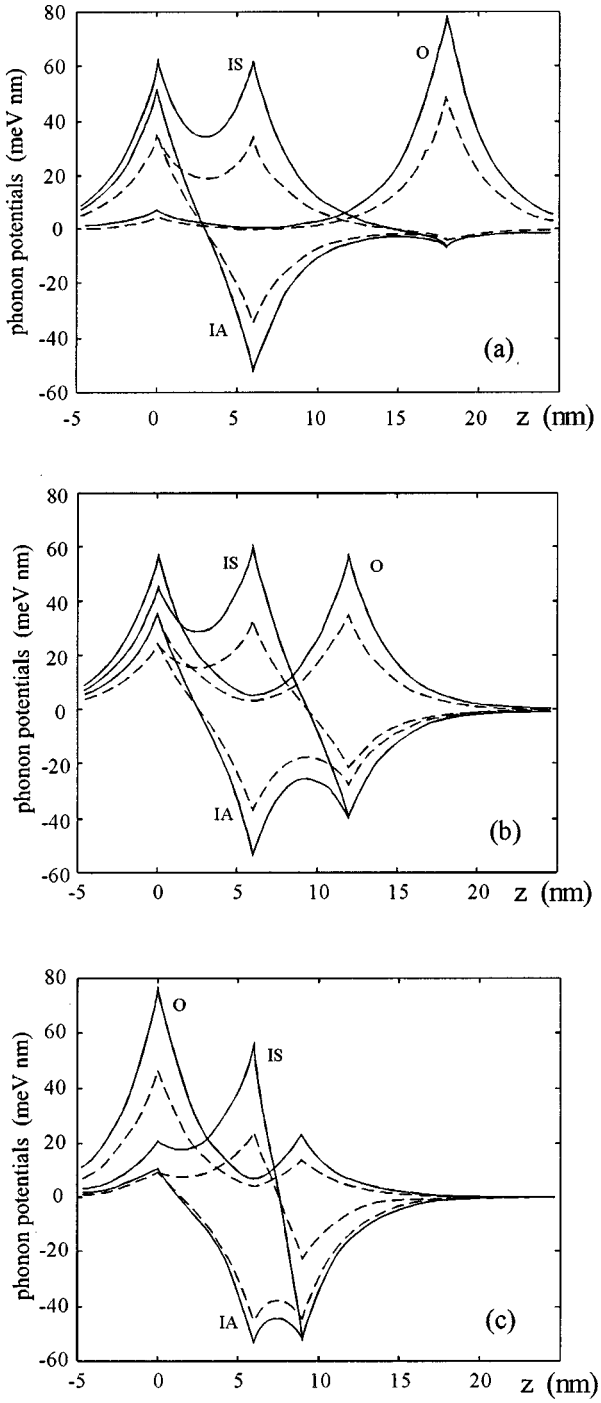

FIG. 3. Interface phonon potential distributions, $e\varphi_m(z)$, calculated for the three-interface heterostructures with different barrier widths: **(a)** $b=12$ nm; **(b)** $b=6$ nm; **(c)** $b=3$ nm. Quantum well width is $a=6$ nm; the value of phonon wave vector q is fixed at 0.4 nm^{-1}. Solid (dashed) lines refer to phonon modes in barrier (well) phonon energy range.

grals between the phonon potential and electron wave functions significantly influence the scattering rates and should be calculated with great care. Since the inclusion of the subband nonparabolicity is essential for the correct description of electron states, we calculate the electron energy spectrum on the basis of the four-band Kane model taking into account the complex boundary conditions for multicomponent wave functions.[18] The calculations have been restricted to the case of a quantum well with a square well potential profile and a

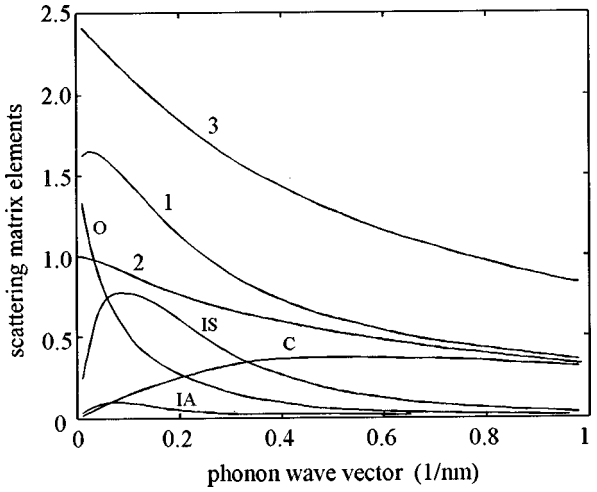

FIG. 4. Scattering rates by the interface phonon modes as functions of the barrier width b at room temperature: **(a)** intrasubband 2–2 transitions; **(b)** intersubband 2–1 transitions. Initial electron kinetic energy in 2nd subband is $E_2=60$ meV. The combined scattering rates by both GaAs-like and AlAs-like modes are represented here.

well width, $a=6$ nm. We use this electron energy spectrum for all scattering rate calculations represented here neglecting the perturbing action of heterointerface (3) onto the electron wave functions in the quantum well. For barrier width $b>2$ nm, this approximation is quite reasonable due to the high energy band offsets $\Delta_{c,v}$ at the AlAs/GaAs heterointerface and, consequently, due to the small penetration of the electron wave function into the barrier region even for high-energetic states in the second subband.

III. SCATTERING RATES

For a heterostructure with large barrier width $b \gg a$, the rates for intrawell scattering processes should be close to the rates in a single quantum well. Parity-selection rules for inner interface mode scattering hold strictly in this limit. Thus, symmetric inner interface and even-parity confined modes dominate in the intrasubband scattering, whereas antisymmetric inner interface and odd-parity confined modes contribute primarily to the intersubband transitions. For large b, the outer interface mode locates at the remote heterointerface (3) and cannot participate in intrawell electron transitions because of the small overlap with the electron states. However, if the well and barrier layer dimensions are comparable, the outer mode scattering becomes dominant in accordance with growing overlap integral and as a result of the higher coupling constant. Correspondingly, the scattering rates by the inner interface modes diminish since these modes switch to the barrier layer. Figure 4 illustrates this behavior for intrasubband 2–2 and intersubband 2–1 electron transitions. Here, scattering rates by interface optical phonons are represented as functions of the barrier width. The scattering rate is computed using the Fermi golden rule. The electron kinetic energy has been chosen so that $E_2=60$ meV in order to include the interaction with all possible interface modes. Figure 5 shows the energy dependence of the total intrasubband 1–1 scattering rates for heterostructures with $b=3$, 6, and 12 nm (curve 1). It is readily seen that the previously mentioned

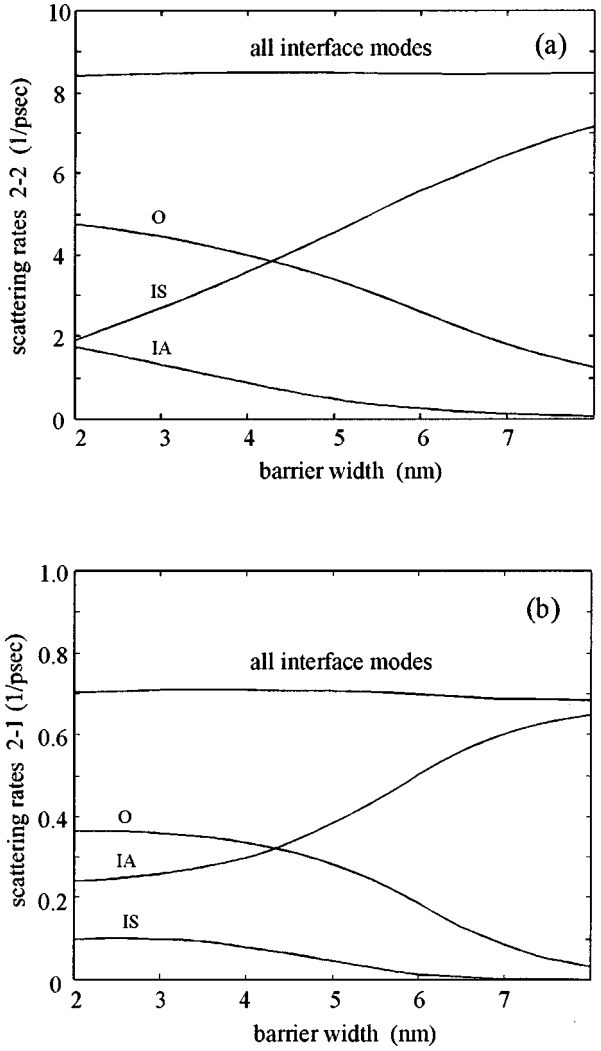

FIG. 5. Total scattering rates for intrasubband 1–1 transitions as function of electron kinetic energy in different phonon spectrum models. For the case when all the interface and confined modes of the heterostructure are taken into account, the curves are labeled by values of the barrier width $b=3$, 6 and 12 nm.

mutual redistribution of the outer and inner phonon modes makes the total interface phonon scattering rate practically independent of barrier width over the entire range of electron kinetic energy.

A qualitative explanation of this result may be related to the sum rule established for the electron–phonon interaction in heterostructures.[3,12,19] Inasmuch as the wave functions of initial and final electron states are confined in the same layer of the heterostructure (quantum well layer in this case) we can divide the total of the squared matrix elements for the scattering processes into two parts, corresponding to the interaction with the interface and confined phonons:

$$\sum_{\text{all modes}} |M_m|^2 = \sum_{\text{interface}} |M_i(a,b)|^2 + \sum_{\text{confined}} |M_c(a)|^2 = \sum_{\text{bulk}} |M_b(a)|^2 \quad (10)$$

Neglecting the phonon energy dispersion, this total should be the same for any complete and orthogonal set of phonon modes; in particular, it equals the sum of matrix elements of the interaction with effective LO bulk phonons. However, for confined electron states, neither the second sum nor the right-hand side of Equation (10) depends on the barrier width b because of the strong damping of electron states in the barrier region. Consequently, we can expect the first sum (for interface modes) to be independent of b as well. It is worth emphasizing that for the interwell or the phonon assisted escape processes the situation can be quite different especially in the case of resonance transitions.[5,15] Here, the proper design of the phonon potential distribution for a given barrier width may appear necessarily to achieve high subband depopulation rate.

For injected and/or hot electrons in the active quantum well of the laser heterostructure, the electron kinetic energy is usually comparable with the LO phonon energy. The condition $E_{kin} \approx \hbar\omega_{ph}$ separates active and passive regions in accordance with the optical phonon emission process and determines the electron distribution function in the low-concentration limit.[20] It is important to realize that just in this electron energy range we cannot substitute the complex phonon spectrum of the heterostructure with bulk phonons of any constituent material. In Fig. 5 we compare the intrasubband 1–1 scattering rates calculated for three different phonon spectrum models. Here, curve 1 represents the total scattering rate due to the combined action of all interface, confined, and barrier phonon modes in the heterostructures with different values of barrier width, b. Two other curves have been obtained by approximating the complex phonon spectrum of the heterostructure with bulk phonons of well (curve 2) or barrier (curve 3) material. In the electron energy range where the phonon energy is crucial for the scattering rate value, the results of the three models differ significantly. Only if the electron kinetic energy exceeds the highest phonon energy in the system can we use the quasibulk approximation suggesting some intermediate composition for the effective bulk semiconductor material.[19] The basis of this approximation is that the total of the matrix elements always falls between the corresponding values for bulk well and bulk barrier materials;[12] this situation is illustrated in Fig. 6. It is seen, however, that this total is substantially different for different values of the phonon wave vector q. Therefore, since the emission scattering rates for different phonon modes depend on the phonon energy stepwise, we cannot choose the unique effective quasibulk approximation in the whole range of different scattering processes and have to use a more complex phonon spectrum. In this article, we have shown that for the three-interface heterostructures, an adequate model of the phonon spectrum is given by the phonon spectrum of a single quantum well.

IV. CONCLUSIONS

Polar electron–optical–phonon interaction in an asymmetric three-interface heterostructure—quantum well plus adjusted barrier layer of finite width, b—has been studied. The interface phonon spectrum of this system is found to consist of three basic types of modes. Two of the interface modes in the limit of the large barrier width can be related to

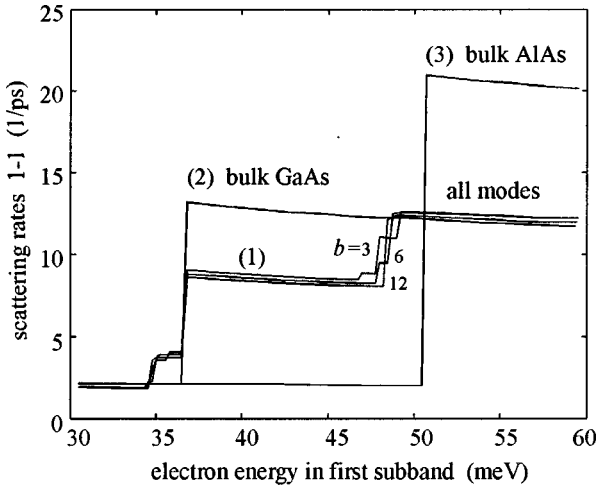

FIG. 6. Scattering matrix elements as functions of phonon wave vector q for intrasubband 1–1 transitions. The sum of all matrix elements **(1)** falls between the corresponding values for bulk well **(2)** and bulk barrier **(3)** phonons. All matrix elements are normalized to the value of bulk GaAs matrix element at small q. Initial electron kinetic energy in the 1st subband is $E_1=60$ meV. Abbreviations: IS(A)—inner symmetric (antisymmetric) interface mode; O—outer interface mode; C—the total of barrier and well confined modes.

symmetric and antisymmetric solutions for an isolated quantum well and have similar dispersion. The third interface mode represents a symmetrized linear combination of single interface modes of the outer heterointerfaces. We have shown that the individual phonon potential distributions in the three-interface heterostructure are substantially modified when changing layer dimensions. The decrease of the barrier width, b, gives rise to the redistribution of the outer interface mode potential from the right outer interface (between barrier layer and half-space narrow gap semiconductor) toward the left outer interface (between barrier half-space and well layer). At the same time, both inner phonon modes switch to the barrier layer simultaneously changing their symmetry. We have found that this mutual redistribution of interface modes keeps the total electron–optical–phonon scattering rate practically unchanged for initial and final electron states localized in the quantum well region. This enables us to use the simpler phonon spectrum of a single quantum well for the analysis of intrawell electron relaxation in the three-interface heterostructures used in cascade laser design. It is interesting to note that this approximation holds true over the entire electron kinetic energy range, including the region where the difference in energy between GaAs-like and AlAs-like optical phonon modes is crucial for scattering rate values. This fact can be explained from the traditional viewpoint of the sum rule for electron–phonon interaction in heterostructures. The applicability of the sum rule for scattering rate calculation has been examined also by comparing the total scattering rate by all interface and confined optical phonons with the results obtained in the quasibulk approximation for the phonon spectrum. We show that in the case of injected or hot electrons with kinetic energy comparable to the typical energy of optical phonons, the quasibulk approximation cannot be used for accurate calculation of the electron–phonon scattering rates in heterostructures.

ACKNOWLEDGMENT

This work was supported by the US Army Research Office.

APPENDIX

In the dielectric continuum model, the electrostatic potential of an interface polar optical mode satisfies the Laplace equation in each layer i; therefore, the z dependence of the potential envelopes can be represented by the function $f(z)$ from (6). The continuity conditions for the electrostatic potential and the normal component of electrical displacement,

$$f_i(z_i)=f_{i-1}(z_i);\quad \varepsilon_i\frac{\partial}{\partial z}f_i(z_i)=\varepsilon_{i-1}\frac{\partial}{\partial z}f_{i-1}(z_i) \tag{A1}$$

may be then written in a simple matrix form,[16]

$$\begin{bmatrix} 1 & e^{-qd_i} \\ -\varepsilon_i & \varepsilon_i e^{-qd_i}\end{bmatrix}\begin{pmatrix} C_{i,1} \\ C_{i,2}\end{pmatrix} = \begin{bmatrix} e^{-qd_{i-1}} & 1 \\ -\varepsilon_{i-1}e^{-qd_{i-1}} & \varepsilon_{i-1}\end{bmatrix}\begin{pmatrix} C_{i-1,1} \\ C_{i-1,2}\end{pmatrix}, \tag{A2}$$

where $d_i=z_{i+1}-z_i$. The transfer matrix is defined as

$$C_i=Q_i(z_i)C_{i-1}. \tag{A3}$$

After imposing the boundary conditions, $C_{0,1}=C_{3,2}=0$, we obtain the dispersion equation for interface modes,

$$[Q_1(z_1)Q_2(z_2)Q_3(z_3)]_{22}=0. \tag{A4}$$

For a three-interface heterostructure with $\varepsilon_0=\varepsilon_2=\varepsilon_b(\omega)$ and $\varepsilon_1=\varepsilon_3=\varepsilon_w(\omega)$, after some straightforward algebra we arrive at relations (2)–(4).

Potential distributions (6) for interface modes are then easily obtained using boundary condition $C_{0,2}=1$ and relation (A3). The proper normalization of the phonon potentials is achieved through the ordinary quantization procedure for lattice displacements,[9]

$$\mathbf{U}_{m,\mathbf{q}}=\sum_i\left(\frac{\hbar\Omega_i}{2\mu_i\omega_m(q)}\right)^{1/2}\frac{e^{i\mathbf{qr}}}{\sqrt{S}}\mathbf{v}_{m,i}(z)(\hat{a}_{m,\mathbf{q}}+\hat{a}^{+}_{m,-\mathbf{q}}); \tag{A5}$$

$$\sum_i\int_{z_i}^{z_{i+1}}dz|\mathbf{v}_{m,i}(z)|^2=1$$

and the relation between the displacement and the potential fields in the Born–Huang theory

$$\mathbf{E}_{m,i}=-\nabla\left(\frac{e^{i\mathbf{qr}}}{\sqrt{S}}\varphi_{m,i}(z)\right)=\frac{\mu_i}{e_i^*}(\omega_{t,i}^2-\omega_{m,i}^2)\mathbf{U}_{mi}. \tag{A6}$$

Here Ω_i, μ_i, and e_i^* are, respectively, the volume, reduced ion mass and effective charge of the elementary unit cell.

[1] R. Lassnig, Phys. Rev. B **30**, 7132 (1984).
[2] N. Mori and T. Ando, Phys. Rev. B **40**, 6175 (1989).
[3] R. Chen, D. L. Lin, and T. F. George, Phys. Rev. B **41**, 1435 (1990).
[4] J. K. Jain and S. Das Sarma, Phys. Rev. Lett. **62**, 2305 (1989); S. Das Sarma, V. B. Campos, M. A. Stroscio, and K. W. Kim, Semicond. Sci. Technol. **7**, B60 (1992).
[5] M. A. Stroscio, J. Appl. Phys. **80**, 6864 (1996).
[6] M. V. Kisin, V. B. Gorfinkel, M. A. Stroscio, G. Belenky, and S. Luryi, J. Appl. Phys. **82**, 2031 (1997).

[7] J. L. Educato, J.-P. Leburton, P. Boucand, P. Vagos, and F. H. Julien, Phys. Rev. B **47**, 12949 (1993); J. Wang, J.-P. Leburton, Z. Moussa, F. H. Julien, and A. Sa'ar, J. Appl. Phys. **80**, 1970 (1996).
[8] G. Sun and J. B. Khurgin, IEEE J. Quantum Electron. **29**, 1104 (1993).
[9] P. J. Turley and S. W. Teitsworth, J. Appl. Phys. **72**, 2356 (1992); Phys. Rev. B **50**, 8423 (1994).
[10] K. W. Kim, A. R. Bhat, M. A. Stroscio, P. J. Turley, and S. W. Teitsworth, J. Appl. Phys. **72**, 2282 (1992).
[11] K. Huang and B. Zhu, Phys. Rev. B **38**, 13377 (1988).
[12] H. Rucker, E. Molinari, and P. Lugli, Phys. Rev. B **45**, 6747 (1992); I. Lee, S. M. Goodnick, M. Gulia, E. Molinari, and P. Lugli, *ibid*. **51**, 7046 (1995).
[13] A. R. Bhatt, K. W. Kim, M. A. Stroscio, and J. M. Higman, Phys. Rev. B **48**, 14671 (1993).
[14] J. Faist, F. Capasso, C. Sirtori, D. L. Sivco, A. L. Hutchinson, and A. Y. Cho, Nature (London) **387**, 777 (1997).
[15] J. Faist, F. Capasso, C. Sirtori, D. L. Sivco, A. L. Hutchinson, M. S. Hybertsen, and A. Y. Cho, Phys. Rev. Lett. **76**, 411 (1996).
[16] S. G. Yu, K. W. Kim, M. A. Stroscio, G. J. Iafrate, J. P. Sun, and G. I. Haddad, J. Appl. Phys. **82**, 3363 (1997).
[17] K. W. Kim and M. A. Stroscio, J. Appl. Phys. **68**, 6289 (1990).
[18] M. V. Kisin, Semiconductors **30**, 928 (1996); **28**, 1143 (1994); **27**, 274 (1993).
[19] L. F. Register, Phys. Rev. B **45**, 8756 (1992).
[20] S. E. Esipov and Y. B. Levinson, Adv. Phys. **36**, 331 (1987).